

FINGERPRINT PATTERN CLASSIFICATION

MASAHITO KAWAGOE and AKIO TOJO

Electrotechnical Laboratory, 1-1-4 Umezono, Tsukuba Science City, Ibaraki 305, Japan

(Received 8 June 1983; in revised form 31 August 1983; received for publication 24 October 1983)

Abstract This paper presents a new method for fingerprint classification. In this method, fingerprint images are divided into 32×32 subregions to obtain direction pattern. Next, the relaxation smoothing process with singularity detection and convergency checking is performed. Starting from the singular regions found, feature parameters of the fingerprint are obtained by extracting major flow-line* traces. The result of the experiments shows that this approach is capable of classifying fingerprint patterns into more than ten categories.

Fingerprint classification
 Syntactic singularity detector

Relaxation smoothing
 Poincaré index

Feature extraction

1. INTRODUCTION

Recently, the need for automatic person identification is increasing more and more in every part of business and industry. Recognizing fingerprints can be one of the most powerful methods for the identification of individuals, and painless for users if an inkless input equipment is employed.⁽¹⁾

There are some systems proposed for precise interpretation of fingerprints based on ridge-line and minutiae analysis, which may be employed, for example, in criminal investigation.^(2,3) This paper presents an automatic fingerprint classification method to assist person identification, which is usually done by identification cards or some similar methods.

There are two main approaches in classifying fingerprints, as follows.

(1) The method based on the shape of ridge lines.^(4,5) In this method the flow of the ridge lines is encoded first. Next, the representative flow-line traces are extracted by analyzing encoded ridge shape. Finally, the fingerprints are classified according to the shape of these flow-lines. Because the method utilizes the global information of a fingerprint, it is robust against missing feature points (e.g. core point, whorl point, delta point) (cf. Fig. 1).

(2) The method based on the feature points.^(6,7) Regarding a fingerprint image as a vector-field, the feature points, such as whorl points or delta points, can be detected with some operations on this field. After this operation, fingerprints are classified by the positions and the kinds of the feature points. Because only the local information of a fingerprint is used in this method, it usually suffers from the weakness

caused by missing delta points, although the process itself is efficient.

In the method described in this paper, we find feature points in a given fingerprint during the noise reduction process.⁽⁸⁾ After coarse classification by these feature points, we obtain major flow-lines by tracing the flow of the direction pattern of the fingerprint. Finally we classify the given fingerprint pattern according to the shape of these flow-lines.^(9,10)

2. NOISE REDUCTION AND SINGULAR AREA DETECTION

In the system described in this paper, a fingerprint is input as a 512×512 binary image and converted into an array of directional patterns composed of 32×32 subregions, each corresponding to a 16×16 pixel area. The average direction of each subregion is estimated by counting micropatterns of image boundaries and represented by four directional components, as explained in Appendix 1.⁽¹¹⁾ The outline of the overall procedure is illustrated in Fig. 2.

2.1. Noise reduction with relaxation method

To eliminate noise components and to detect singularity, defined in the next section, the relaxation process is applied to the directional pattern described above, as follows.⁽¹²⁾

Repeat 4 times

if (x is singular or converged) **and** (not first 2 times of this process)

then $P(r, x, n + 1) = P(r, x, n + 1)$

else $q(r, x) = \sum_{x' \in N(x)} \sum_{r'} C(r, r') P(r', x', n)$

$$P(r, x, n + 1) = [1 + q(r, x)] P(r, x, n) / \sum_r [1 + q(r, x)] P(r, x, n)$$

* We use the term 'flow-line' to designate curves extracted from a coded fingerprint image, as shown in Fig. 15 or Fig. 18. It is different from 'ridge lines' in the original image.

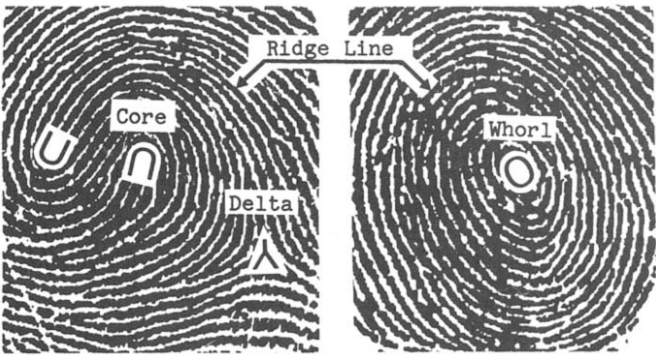


Fig. 1. Definition of fingerprint features.

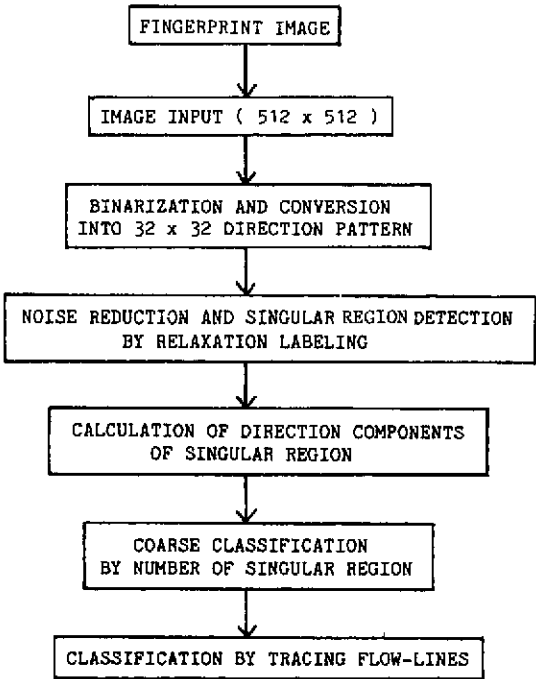


Fig. 2. Outline of the fingerprint classification process.

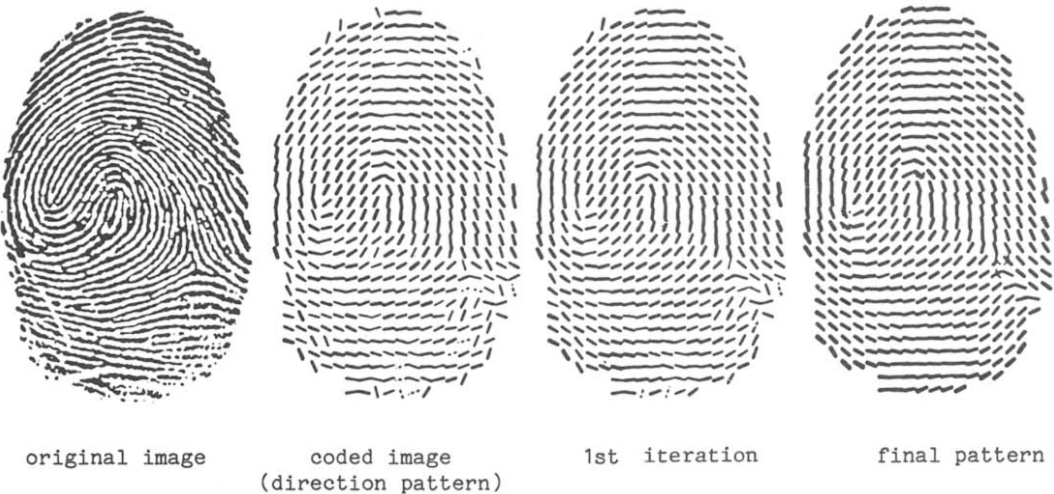


Fig. 3. An example of noise reduction. The thickness of a line shows the reliability of the direction.

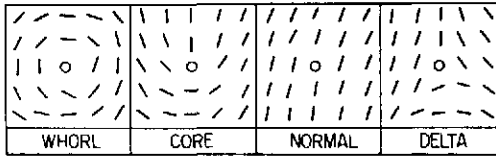


Fig. 4. Four types of flow patterns.

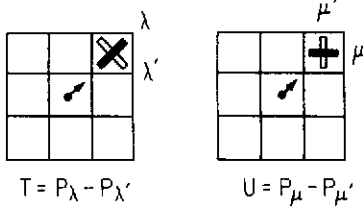


Fig. 5. Definition of T and U .

(P_λ is the probability of the direction component λ obtained by the method described in Appendix 1.)

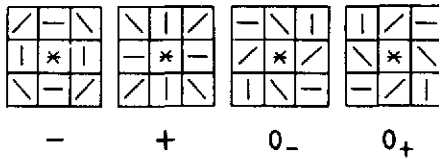


Fig. 6. Flow code and corresponding pattern.

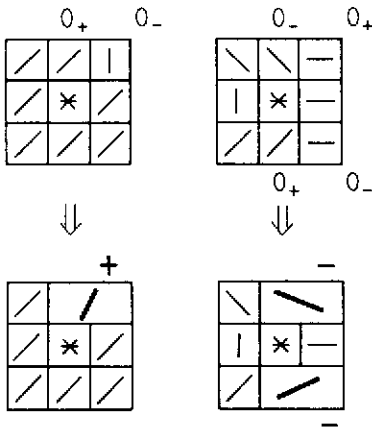


Fig. 7. Examples of applying Rule (1) and Rule (2).

Table 1. Flow code assignment rule

| Condition | Code |
|------------------------------|------------------|
| $0.1 < T$ | $\Rightarrow +$ |
| $0.1 > T > -0.1$ and $U > 0$ | $\Rightarrow 0+$ |
| $0.1 > T > -0.1$ and $U < 0$ | $\Rightarrow 0-$ |
| $-0.1 > T$ | $\Rightarrow -$ |

where

$P(r, x, n)$ is the probability of direction r at position x in the n th iteration,

x, x' is the subregion's position,

r, r' is the direction component ($0^\circ, 45^\circ, 90^\circ, 135^\circ$)

$C(r, r')$ is the compatible coefficients

$= 1$ when r is parallel to r'

$= -1$ when r is perpendicular to r'

$= 0$ otherwise,

$N(x)$ is the 8-neighbors of x ,

converged is the sum of the probabilities of two adjacent direction components > 0.9 ,

singular is determined by the process described in section 2.2.

An example of the relaxation process is shown in Fig. 3. We remove the converged or singular subregions from the relaxation process because (1) we want to preserve true directional information by avoiding overconvergence to one of the four directions, and (2) at the singular subregions which correspond to the feature points in Section 1, direction cannot be defined in nature.

2.2. Singular region detection

2.2.1. Singularity detection by label-structure method.

There are four types of neighborhood flow pattern around each subregion, as shown in Fig. 4. Subregions which are not normal are defined as singular and correspond to the feature points described in Section 1. To obtain the flow pattern around each subregion, the following steps are performed. First, the whorlness at each subregion is determined by calculating T and U , shown in Fig. 5. Next, the flow codes are assigned to these subregions using the assignment rule shown in Table 1. Figure 6 shows the nature of the flow code. An example of assigned flow codes is shown in the first line of Fig. 8.

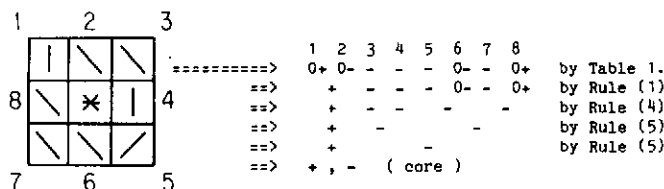


Fig. 8. An example of the rewriting process.

Table 2. Decision rule of singularity type

| Label | Type |
|------------------|-----------------------------|
| - | Whorl |
| +, - | Core |
| +, -, +, - | Normal |
| +, -, +, -, +, - | Delta |
| + | Not existent in fingerprint |

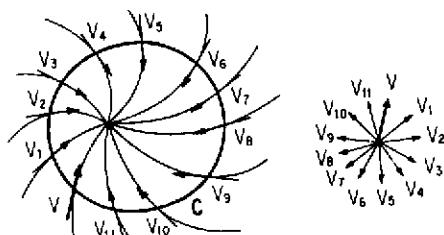
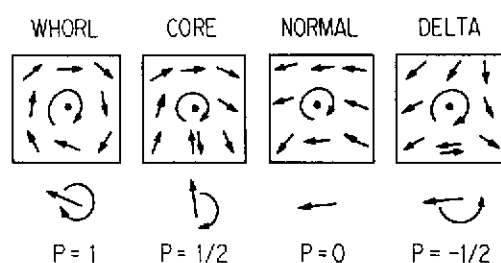
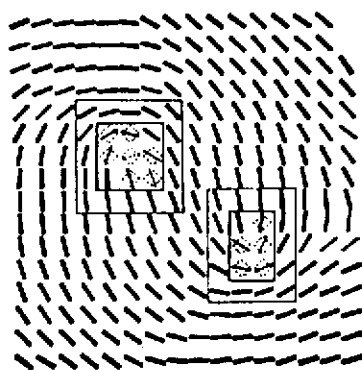
Fig. 9. Definition of Poincaré index. The index is defined as an amount of rotation of the vector V along the curve C .

Fig. 10. Singular point and its Poincaré index.

Fig. 11. An example of singularity check by Poincaré index. (\odot denotes singular subregions.)

At the next step, the flow codes are rewritten according to the following rewriting rules:

- (1) $0+, 0- \Rightarrow +$
- (2) $0-, 0+ \Rightarrow -$
- (3) $+, 0* \Rightarrow +$ (* denotes don't care condition)
- (4) $-, 0* \Rightarrow -$
- (5) $+, + \Rightarrow +$
- (6) $-, - \Rightarrow -$
- (7) $0+, 0+ \Rightarrow 0+$
- (8) $0-, 0- \Rightarrow 0-$

where the codes are observed clockwise and rule (1) and rule (2) are applied before rules (3)–(8). Figure 7 shows the case where rule (1) or rule (2) holds. Rules (1) and (2) are applied simultaneously, so that $(0-, 0+)$, for example, is changed to $(-, +)$. An example of the rewriting process is shown in Fig. 8. At the final step of the rewriting process, the codes are merged into one of the states shown in Table 2, and the types of singularity are determined using this information.

2.2.2. Singularity verification by Poincaré index and coarse fingerprint classification. Poincaré index, shown in Fig. 9, is useful to check singularities in a fingerprint pattern, as in the case of a field described by a differential equation.⁽¹³⁾ In order to limit the area of the singular region, the subregions which are estimated to be singular by the label-structure method described in the previous section are checked by Poincaré index, as illustrated in Fig. 10. As the field of a fingerprint is bidirectional, we select a direction of the flow of each subregion so that it is nearer to the direction of adjacent regions along the path. The method is essentially the same in principle as the one presented by Chang.⁽¹⁴⁾

After checking the singularity of each subregion, we define singular regions as minimum enclosing rectangles which contain connected singular subregions with the same singularity type. They are classified into four categories, again using Poincaré index calculated around the periphery of each singular region, as illustrated in Fig. 11. Then fingerprints can be classified coarsely by the number of whorls, cores and deltas obtained in the above process. The classification rules are shown in Table 3.

3. FINE CLASSIFICATION BY FLOW TRACING

The number of cores and deltas are not enough for detailed classification of fingerprints. Parameters for

Table 3. Coarse classification by singular region count

| Whorl | Core | Delta | Type |
|-------|------|-------|-------------------------------------|
| 1 | 0 | * | Whorl |
| 0 | 1 | * | Loop, pocketed loop, or tented arch |
| 0 | 2 | * | Twin loop or whorl |
| 0 | 0 | 0 | Arch |

* Don't care

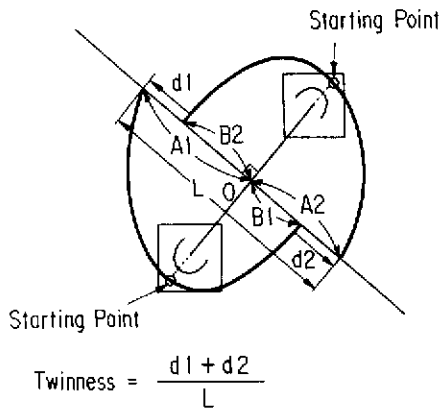


Fig. 12. Parameters obtained by flow-line tracing.

fine classification are obtained by flow-line tracing around the singular regions, as described below.

3.1. Discrimination between twin and whorl

First, we consider the major group which is classified into whorl-twin type. As illustrated in Fig. 12, the lengths A1, B1, A2 and B2 are obtained from flow-line traces starting from the singular regions to the perpendicular bisector. Whorl type and twin type are discriminated by the rules shown in Fig. 13 and three parameters A1/B2, A2/B1 and the flow direction at the center.

Although clear whorl type and twin type are distinguishable using the above parameters, actual

fingerprint patterns are continuously distributed between twin and whorl and are sometimes very difficult to discriminate, even for a person. We, therefore, define another two parameters which can describe both twin and whorl type uniformly and quantitatively. The first parameter is twinness, defined as the amount of the difference between two flow-lines, as shown in Fig. 12. This parameter indicates the following:

twinness > 0: twin convoluting counterclockwise,
nearly zero: whorl,
twinness < 0: twin convoluting clockwise.

The other parameter is the flatness, defined from the ellipse which fits on two flow-lines, as illustrated in Fig. 14. The ratio of the short to the long diameter is used to describe the flatness of the given pattern. Figure 15 shows an example of flow-lines to obtain these parameters.

Figure 16 is a plot of whorl and twin type patterns based on these two parameters, showing that the classification at dotted lines in the figure is consistent with the classification by the rules given in Fig. 13. Consequently, these two parameters are considered to be pertinent as common parameters for twin and whorl type discrimination.

3.2. Discrimination between loop and pocket

When a given fingerprint is classified as a single core type at the coarse classification stage, it is further classified by the following steps.

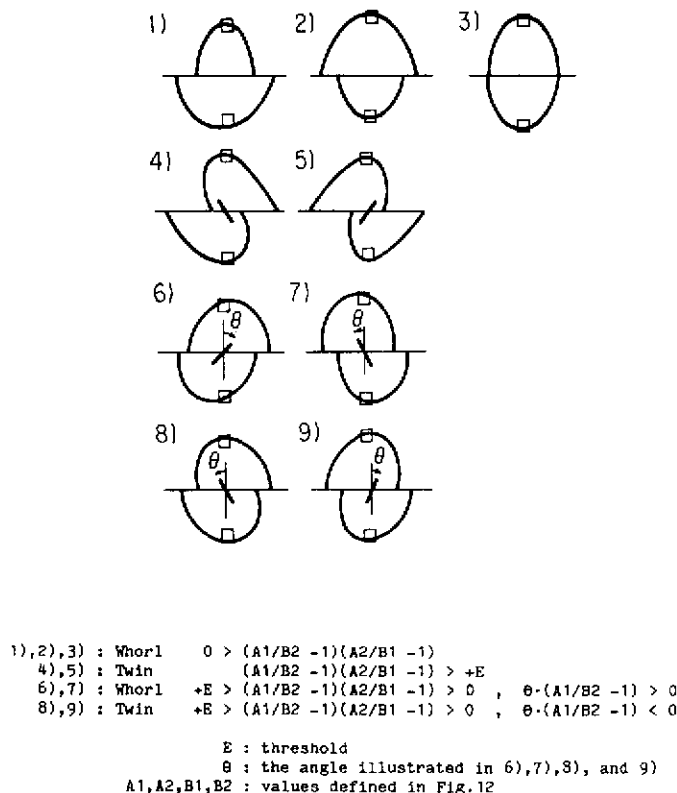


Fig. 13. Whorl and twin discrimination rule.

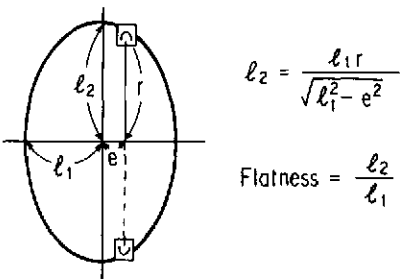


Fig. 14. Definition of flatness.

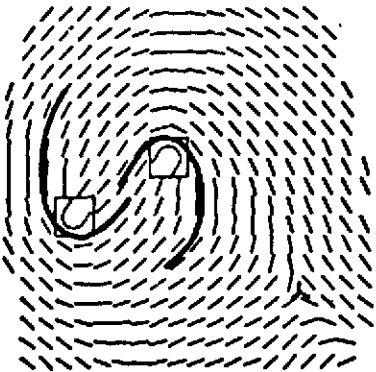


Fig. 15. An example of traced flow-lines.

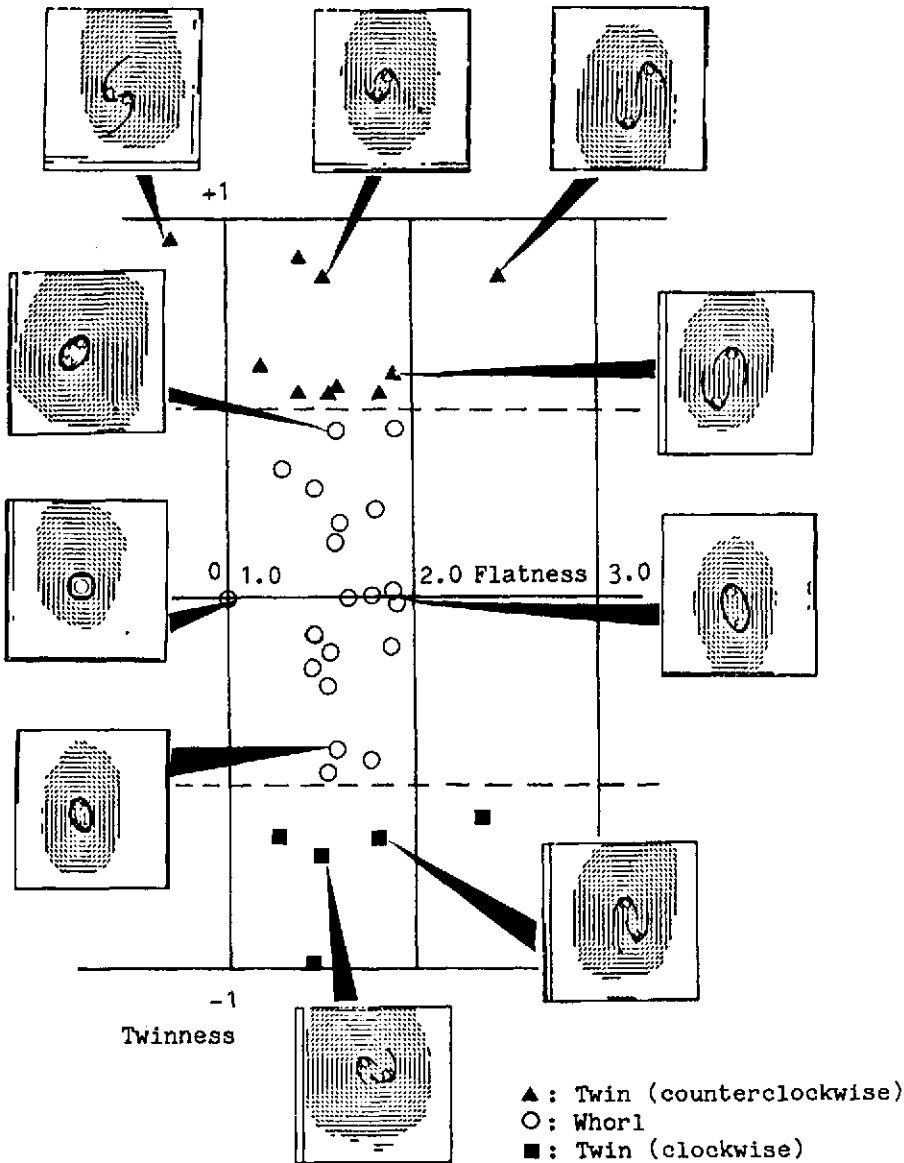


Fig. 16. Twins and whorls on twinness-flatness space.

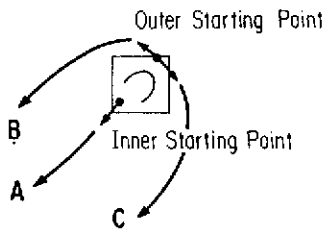


Fig. 17. Trace for loop and pocketed loop type.

At the first step, the fingerprint is classified into one of the three classes according to the inclination of the central trace, shown in Fig. 17:

- (1) left-loop or left-pocketed loop type (left-downward);
- (2) right-loop or right-pocketed loop type (right-downward);
- (3) tented arch type (vertical).

At the next step, distinction between loop type and pocketed loop type is performed using the central trace and the other two flow-line traces obtained by tracing from the inner side and outer side of the singular region. If the central trace meets one of the side lines, the fingerprint is classified as pocketed loop type. Otherwise it is classified to be loop type.

If the position of the fingers can be fixed, the fingerprint will be classified more finely using the amount of inclination of the central trace as a classification parameter.

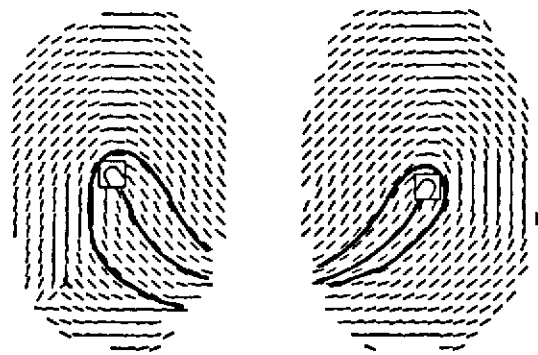
Examples are shown in Fig. 18.

4. RESULT AND CONCLUDING REMARKS

A fingerprint classification experiment based on the proposed method is carried out on 94 fingerprint samples taken with an inkless input device.⁽¹⁵⁾ (see Appendix 2)

The fingerprints are classified into seven coarse classes, and twin and whorl types are further classified by the two parameters defined in Section 3. Table 4 summarizes the results of the experiment.

Discrimination between twin type with close cores and whorl type with divergence is not clear from the information condensed into 32×32 direction patterns. On the other hand, however, this fact indicates that these two types should be classified together within the same category by flatness and twinness characteristics.



a) Right Loop

b) Left Pocket

Fig. 18. Examples of loop and pocketed loop.

To put the system into practical use, we will have to check the reproducibility of classification results. We also have to devise some method to fix the finger position and other input conditions. If these conditions are satisfied, we will also be able to classify the loop, pocket and tented arch type finely using the angle of the central flowline.

SUMMARY

This paper presents an automatic fingerprint classification method to assist person identification, which is usually done by identification cards or some similar method. The method is summarized as follows.

- (1) Data compression by direction pattern. Fingerprint images are divided into 32×32 subregions to obtain direction pattern. Direction pattern is made from the histogram of micropatterns in each subregion.
- (2) Relaxation smoothing. The relaxation smoothing process with singularity detection and convergency checking is performed. The converged or singular points are omitted from the normal relaxation process in order to avoid overconvergence to one of the four direction components and assignment of a false direction to the points where direction cannot be defined in nature.
- (3) Poincaré index check. The singular points detected in the above process are re-examined by a Poincaré index obtained from the surrounding areas. The fingerprint is coarsely classified by the numbers of the singular points.

Table 4. Results of experiment

| | Left loop | Right loop | Left pocket | Right pocket | Whorl & twin (Fig. 16) | Arch & tented | Irregular | Total |
|-------|-----------|------------|-------------|--------------|------------------------|---------------|-----------|-------|
| Right | 11 | 14 | 0 | 1 | 59 | 0 | 1 | 86 |
| Wrong | 2 | 3 | 0 | 0 | 3 | 0 | 0 | 8 |
| Total | 13 | 17 | 0 | 1 | 62 | 0 | 1 | 94 |

| | |
|--------|--|
| type 1 | |
| type 2 | |
| type 3 | |
| type 4 | |
| type 5 | |

Fig. 19. Five types of micropattern.

(4) Major tracelines for fine classification. Feature parameters for fine classification of the fingerprint are obtained extracting major flow-line traces, starting from the singular regions found.

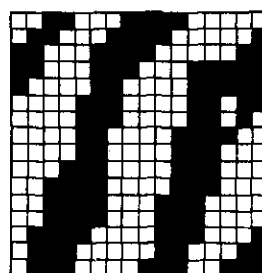
An experiment based on the proposed method was carried out on 94 fingerprints samples taken with an inkless input device. The results of the experiment show that the method can be employed in practical person identification applications.

Acknowledgement—The authors wish to thank Mr. Tetsuro Yamaguchi of the Electrotechnical Laboratory for his valuable cooperation and helpful suggestions on the method to obtain the direction pattern.

They also thank Mr. Takanoki Sato, the chief of the Information Systems Section, and other members of the same section, for valuable discussions.

REFERENCES

1. A. Tojo, PIPS Report PIPS-R-No. 25, pp. 63–64, Electrotechnical Laboratory (1980) (in Japanese).
2. K. Asai, S. Hiratsuka and Y. Hoshino, Identification of poor quality fingerprints, *Trans. IECE J65-D*, 618–624 (1976) (in Japanese).
3. W. J. Hankley and J. T. Tou, Automatic fingerprint interpretation and classification via contextual analysis and topological coding, *Pictorial Pattern Recognition*, G.



type 1 = 2
type 2 = 58
type 3 = 32
type 4 = 2
type 5 = 1

- C. Cheng, R. S. Ledley, D. K. Pollock and A. Rosenfeld, eds. Thompson Book Company (1968).
4. B. Moayer and K. S. Fu, A syntactic approach to fingerprint pattern recognition, *Pattern Recognition* 7, 1–23 (1975).
5. K. Rao and K. Balck, Type classification of fingerprints: a syntactic approach, *IEEE Trans. Pattern Anal. Mach. Intell.* PAMI-2, 223–231 (1980).
6. S. Ohteru, H. Kobayashi, T. Kato, K. Tamayama and F. Noda, Automated fingerprint processor, IECE Technical Report IT 73-4 (1973) (in Japanese).
7. K. Goto, O. Kakamura, T. Minami and H. Okuno, Fingerprint classification by distribution pattern of ridge directions, IECE Technical Report IE 81-88 (1981) (in Japanese).
8. M. Kawagoe, A. Tojo and T. Yamaguchi, Classification of fingerprint patterns by relaxation method, *IPSJ 22nd National Conf.*, p. 3D-8 (1981) (in Japanese).
9. M. Kawagoe and A. Tojo, Automatic classification of fingerprint patterns, *IPSJ 24th National Conf.*, p. 4E-10 (1982) (in Japanese).
10. M. Kawagoe and A. Tojo, Automatic classification of fingerprint patterns, IPSJ Technical Report on Computer Vision, Vol. 18-2 (1982) (in Japanese).
11. T. Yamaguchi and A. Tojo, A fingerprint coding method, *IECE National Conf.*, 1086 (1979) (in Japanese).
12. A. Rosenfeld, Iterative method in image analysis, *Proc. IECE National Conf.*, p. 1086 (1979) (in Japanese), pp. 14–18 (1977).
13. R. Rosen, *Dynamical System Theory in Biology*, Vol. 1. John Wiley, New York (1970).
14. T. L. Chang, Texture analysis of digitized fingerprints for singularity detection, *Proc. Int. Joint Conf. on Pattern Recognition*, pp. 478–480 (1980).
15. T. Yamaguchi, An input equipment for surface patterns, Japanese Patent Application No. 85184 (1978).

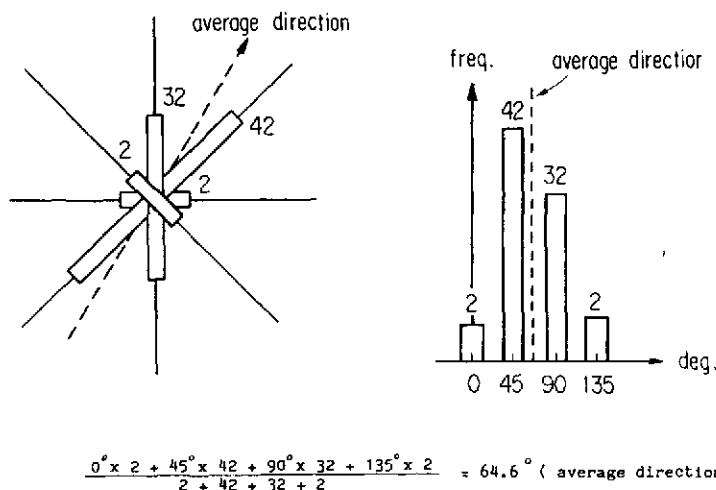


Fig. 21. Direction represented by quadruplet.

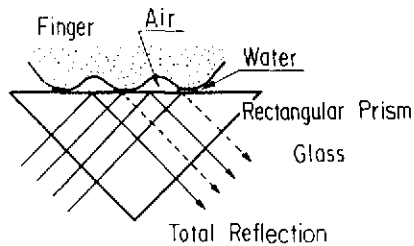


Fig. 22. Input equipment based on total reflection.

APPENDIX 1. METHOD FOR OBTAINING DIRECTION PATTERN FROM A MICROPATTERN HISTOGRAM

For each 32×32 subregion, we obtain a histogram of five types of micropatterns, shown in Fig. 19, corresponding to 0 degrees, 45 degrees, 90 degrees and 135 degrees components, and an undefined direction component. In the case of the subregion of Fig. 20, we find two type 1, 58 type 2, 32 type 3, two type 4 and one type 5 micropatterns, respectively.

In this encoding method, we make no distinction between black pattern and white pattern, and so it is not possible to decide to which direction of 45 degrees or 135 degrees the type 5 micropatterns should be classified. Therefore, we regard the type 5 micropatterns as belonging to both type 2 and type 4 (consider a checker board pattern for example). We also have to divide the count of type 2 and type 4 micropatterns by $\sqrt{2}$ in order to compensate over-estimation in the direction of 45 and 135 degrees. Finally, we obtain a quadruplet by which we represent the direction of each subregion as shown below (numerical values correspond to the example shown in Fig. 20).

$$\begin{aligned}
 (\text{type 1, type 2, type 3, type 4, type 5}) &= (2, 58, 32, 2, 1) \\
 \Rightarrow (0 \text{ degrees, } 45 \text{ degrees, } 90 \text{ degrees, } 135 \text{ degrees}) & \\
 &= (2, 42, 32, 2)
 \end{aligned}$$



Fig. 23. Examples of an input image from the inkless input device.

We can define the average direction of a subregion from this quadruplet, as shown in Fig. 21, and therefore we can represent any direction continuously by this quadruplet.

APPENDIX 2. AN INKLESS FINGERPRINT INPUT METHOD

We use equipment based on the total reflection phenomenon, as illustrated in Fig. 22. Figure 23 shows a typical input image obtained using this equipment.

The image of a fingerprint is deformed, because a finger is located obliquely to the optical axis of the equipment, as shown in Fig. 22. The deformation is corrected at the preprocessing stage, before the image is converted to a direction pattern.

About the Author—MASAHIRO KAWAGOE received the B.E. and M.E. degrees at the University of Tokyo, in 1975 and 1977, respectively. He has worked in the Computer Science Division of the Electrotechnical Laboratory since 1977. His research interests include relaxation method, pattern recognition and image understanding. He is a member of the Information Processing Society of Japan, the Society of Instrument and Control Engineers and the IECE of Japan.

About the Author—AKIO TOJO received the B.E., M.E. and Dr. of Eng. degrees at the University of Tokyo, in 1960, 1962 and 1966, respectively. Since 1966 he has been with the Electrotechnical Laboratory. His research interests include pattern recognition, image understanding, interactive systems and computer architectures. Dr. Tojo is currently the head of the Computer Science Division of the Electrotechnical Laboratory. He is a member of the ACM, the Information Processing Society of Japan, the Society of Instrument and Control Engineers, the IECE of Japan and the Robotics Society of Japan.